Coupled Systems Mechanics, *Vol. 7, No. 2 (2018) 177-195*
DOI: https://doi.org/10.12989/csm.2018.7.2.177

Influence of ductility classes on seismic response of reinforced concrete structures

Željana Nikolić*, Nikolina Živaljić[a] and Hrvoje Smoljanović[b]

Faculty of Civil Engineering, University of Split, Architecture and Geodesy, Matice hrvatske 15, 21000 Split, Croatia

(Received June 29, 2017, Revised August 8, 2017, Accepted August 17, 2017)

Abstract. Reinforced concrete buildings in a seismically active area can be designed as DCM (medium ductility) or DCH (high ductility) class according to the regulations of Eurocode 8. In this paper, two RC buildings, one with a wall structural system and the other with a frame system, previously designed for DCM and DCH ductility, were analysed by using incremental dynamic analysis in order to study differences in the behaviour of structures between these ductility classes, especially the failure mechanism and ultimate collapse acceleration. Despite the fact that a higher behaviour factor of DCH structures influences lower seismic resistance, in comparison to DCM structures, a strict application of the design and detailing rules of Eurocode 8 in analysed examples caused that the seismic resistance of both frames does not significantly differ. The conclusions were derived for two buildings and do not necessarily apply to other RC structures. Further analysis could make a valuable contribution to the analysis of the behaviour of such buildings and decide between two ductility classes in everyday building design.

Keywords: ductility classes; Eurocode 8; incremental dynamic analysis; reinforced concrete buildings

1. Introduction

One of the most convenient ways in the design of earthquake resistant structures is determining the seismic effects on the basis of modal response spectrum analysis using linear-elastic behaviour of the structures. The capacity of the structure to dissipate energy is ensured through the application of design spectrum, which represents the elastic response spectrum of ground acceleration reduced by behaviour factor q. This factor is equal for the whole group of structures and gives a rough estimation of its real behaviour. The European standard for earthquake resistance design of the structures (Eurocode 8 2005, further referred to as EC8) allows the design of reinforced concrete buildings (RC buildings) by choosing between two ductility classes with different value of behaviour factor, DCM (medium ductility) and DCH (high ductility), depending on their hysteretic dissipation capacity. In order to provide the appropriate amount of ductility,

*Corresponding author, Professor, E-mail: zeljana.nikolic@gradst.hr
[a]Assistant Professor, E-mail: nikolina.zivaljic@gradst.hr
[b]Assistant Professor, E-mail: hrvoje.smoljanovic@gradst.hr

Copyright © 2018 Techno-Press, Ltd.
http://www.techno-press.org/?journal=csm&subpage=8 ISSN: 2234-2184 (Print), 2234-2192 (Online)

specific provisions for all structural elements ought to be met in each class. Due to the requirement of a higher behaviour factor, DCH structures are designed for lower lateral strength, but have stringent rules for detailing and strength assessment. Design and detailing rules required for DCM structures are less demanding than for DCH. Therefore, DCH has been little used, and some of its detailing provisions are found hard to achieve in practice (Boot 2014).

Two ductility classes prescribed by EC8 are suggested to predefine the behaviour of structures, leading to different responses. However, the behaviour of the structure cannot be fully predetermined due to many factors that play a key role in such a problem. Specifically, the diversity of the nature of earthquake can produce significant differences in structural behaviour with respect to the same ductility class. Furthermore, each of the ductility classes implies completely different perspective regarding the design of the building. Hence, one needs to make a judicious choice between the two classes balancing between the desired response of the structure, costs and complexity of design and construction.

Powerful numerical models stand as significant tools for obtaining more insight into the particularities of each structure. Moreover, the overall analyses of couple of characteristic earthquakes in terms of DCM and DCH classes of a certain structure can give us a more elaborate answer to this question. The model of this kind should be able to produce highly non-linear effects for realistic description of the structural behaviour under the cyclic loading until the collapse, especially opening and closing of the cracks in concrete, slip of the reinforcing bar due to a high plastic deformation under reversed cyclic loading, as well as yielding and failure of the reinforcement. Incorporating these phenomena in a satisfactory manner ensures realistic modelling of energy dissipation capacity and response of the structure during seismic loading.

Modelling of opening and closing of the cracks caused by cyclic excitation is crucial for realistic modelling of energy dissipation in RC structures and their non-linear dynamic response due to earthquakes. Available non-linear numerical models for time-dependent analysis of RC structures under seismic loading are mostly based on finite element method and smeared crack approach, where the cracked material is represented as a continuum, and local displacement discontinuities are smeared over some tributary areas. A combination of this approach with classical plasticity or damage models can give a relatively good approximation of the global structural response with low computational cost. However, more accurate computation of energy dissipation caused by concrete cracking under the extreme earthquake's excitation can be obtained with discrete crack approach.

The classical modelling approach of discrete cracks in quasi-brittle materials was performed through the framework of finite element method by using cohesive elements across element edges (Ortiz and Pandolfi 1999) or by considering adaptive refinement techniques (Ortiz and Quigley 1991). The other possibility is discontinuum-based modelling where discontinuum state of the structure is assumed a priori, leading to discrete element method (DEM) (D'Addetta *et al.* 1999) with different variations of connections between discrete elements presented through lattice discrete models (Schlangen and Garboczi 1997, Cusatis *et al.* 2006, Nikolic *et al.* 2017a) and rigid body spring models (Yamamoto *et al.* 2014). In the last two decades, an increasing number of models attempted to combine the advantages of continuum and discontinuum-based modelling (Ghaboussi 1997, Pearce *et al.* 2000, Munjiza 2004) where the cracking was considered along the finite element edges. Some approaches are based on the modelling of the discontinuity inside the finite elements through the finite element method with embedded strong discontinuities (ED-FEM method) (Simo *et al.* 1993, Armero and Garikipati 1996, Armero and Linder 2009, Ibrahimbegovic *et al.* 2010, Nam Do *et al.* 2015a, Nam Do *et al.* 2015b), extended finite elements (X-FEM

method) (Moes *et al.* 1999, Wells *et al.* 2002, Rethore *et al.* 2005) or lattice discrete models with strong discontinuity (Nikolic *et al.* 2015, Nikolic and Ibrahimbegovic 2015, Nikolic *et al.* 2016). Microplane model based on the monitoring of stresses in predefined directions, which is similar to discrete models, was also applied in predicting the fracture phenomena (Bažant *et al.* 2000, Ožbolt *et al.* 2001).

The intention of this paper is to give more insight into the failure of RC buildings due to earthquake excitation. Hence, we provide the simulations from two different modelling approaches, namely one based on finite discrete methodology (Živaljić *et al.* 2013, Nikolić *et al.* 2017b) and the other based on finite elements, where material inelasticity and the cross-section behaviour are presented through the fibre approach (SeismoStruct). The goal of both models is to apply the knowledge of influence of ductility classes from EC8 on structural resistance. More precisely, we studied development of damage zones, ultimate bearing capacity and corresponding failure mechanisms on two reinforced concrete buildings with different structural resistant system (wall and frame structural system) using incremental dynamic analysis (Vamvatsikos and Cornell 2002).

2. Input for incremental dynamic analysis

Dynamic response of the buildings in both modelling approaches presented in this paper was conducted by the incremental dynamic analysis (IDA) up to the failure (Vamvatsikos and Cornell 2002). This method is widely used in performance based seismic design (Pramanik *et al.* 2016). The buildings were subjected to a series of realistic earthquake excitations in terms of time-history analyses of increasing intensity (e.g., peak ground acceleration is incrementally scaled from a low elastic response value up to the failure). Careful attention was given to the selection of time-history records in order to satisfy the acceleration spectrum assumed in design.

Seismic loading was represented by horizontal ground acceleration recorded on the soil class B during real earthquakes. The set of seven ground motion records were chosen from the European Strong-Motion according to Iervolino *et al.* (2008). Selected earthquakes are listed in Table 1 and shown in Fig. 1.

Table 1 Selected ground motion records (European Strong-Motion Database)

Event Name	Country	Station name	Code	Date	a_{max}
South Iceland	Iceland	Selsund	004677xa	17/06/2000	0.33 *g*
Montenegro	Montenegro	Bar-Skupstina Opstine	000199ya	15/04/1979	0.44 *g*
Montenegro (aftershock)	Montenegro	Petrovac-Hotel Rivijera	000229ya	24/05/1979	0.33 *g*
Montenegro (aftershock)	Montenegro	Budva-PTT	000230ya	24/05/1979	0.32 *g*
Erzincan	Turkey	Erzincan-Meteorologij Mudurlugu	000535ya	13/03/1992	0.61 *g*
South Iceland	Iceland	Hella	004673ya	17/06/2000	0.57 *g*
South Iceland (aftershock)	Iceland	Kaldarholt	006328ya	21/06/2000	0.47 *g*

The selected accelerograms were scaled by taking into account that maximum value of the

acceleration ought to be $a_g S$, where a_g was design ground acceleration, and S was the soil parameter according to EC8. The acceleration spectra of the selected earthquakes for damping ξ=5%, their average value and Type 1 elastic spectrum for a_g=0.3 g according to EC8 are shown in Fig. 2. Namely, according to the most of the seismic design codes, including EC8, if seven or more time-histories are used in analysis, than the average structural response is valid for the design. The average elastic spectrum of seven selected earthquakes should not drop below the value of 90% of elastic spectrum prescribed by EC8 in any period of the structure. Comparison between average response spectra of selected earthquakes and Type 1 elastic spectrum (Fig. 2) shows that this condition was satisfied.

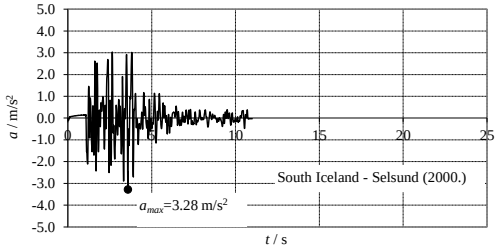

(a) South Iceland - Selsund (Iceland, 2000)

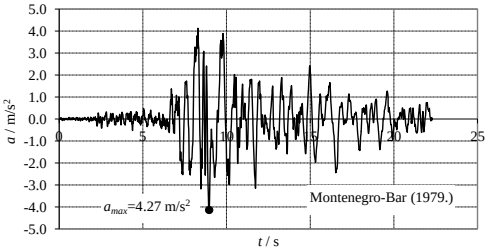

(b) Montenegro - Bar (Montenegro, 1979)

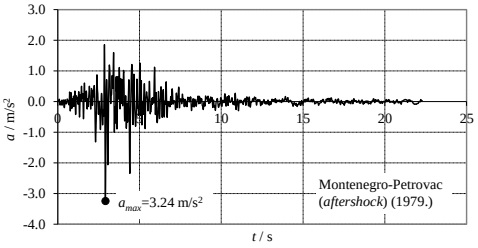

(c) Montenegro (aftershock) -Petrovac (Montenegro, 1979)

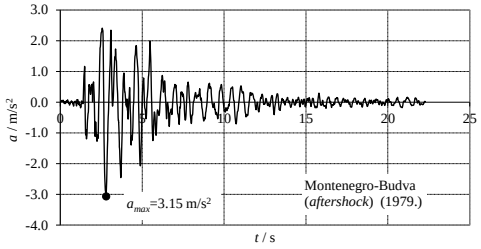

(d) Montenegro (aftershock) - Budva (Montenegro, 1979)

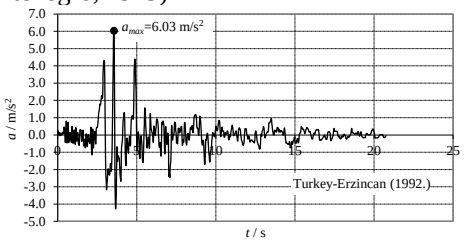

(e) Erzincan (Turkey, 1992),

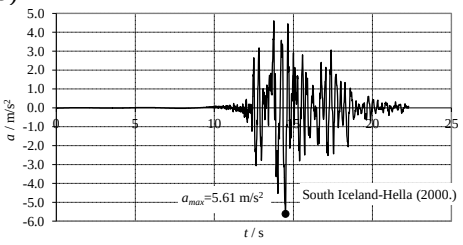

(f) South Iceland - Hella (Iceland, 2000)

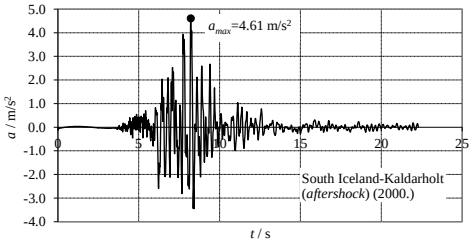

(g) South Iceland (aftershock) - Kaldarholt (Iceland, 2000)

Fig. 1 Earthquake records adopted in the analysis

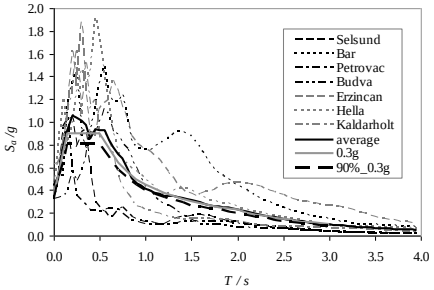

Fig. 2 Response spectra of the selected records, their average value and elastic spectrum (EC8-Type 1)

Using seven modified records, incremental dynamic analysis (Vamvatsikos and Cornell 2002) was performed for analysed RC buildings. Each of the seven records was applied with increasing ground motion intensity up to the failure of the structure.

3. Non-linear analysis of RC building with wall structural system

The non-linear analysis of RC wall structures was performed by finite-discrete element model (Nikolić *et al.* 2017b), which accounts for material non-linearities and discrete cracks representation approach. The accuracy of the model and its performance in modelling the static and dynamic response of RC plane concrete structures has been extensively validated in previous studies (Živaljić *et al.* 2012, Živaljić *et al.* 2013, Živaljić *et al.* 2014, Nikolić *et al.* 2017b). Therefore, only short description of the model is given in the following sections, in order to explain its main characteristics.

3.1 Description of numerical model

The applied model considers discrete representation of the cracks. The concrete structure is discretised on triangular finite elements, whereas the reinforcing bars are modelled with linear 1D elements. The structure is assumed to behave as a linear elastic continuum until the initiation of the cracks and discontinuities, which are allowed to propagate through the joint elements of concrete, leading to the deformation in the reinforcing bar joint elements. The concrete and reinforcing bars are analysed separately, but they are connected by the relationship between the size of the concrete crack and the strain of the reinforcing bar. The model of the 2D RC structure with the embedded reinforcing bar is presented in Fig. 3.

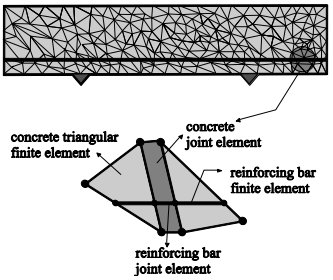

Fig. 3 Discretisation of RC structure

Non-linear numerical model in concrete contact element is used for simulation of crack initiation and propagation in tension and shear. The cracks are assumed to coincide with the finite element edges, which are achieved in advance through the topology of adjacent elements described by different nodes. Separation of these edges induces a bonding stress which is taken to be a function of the size of separation δ (Fig. 4). Before reaching tensile strength, there is no separation of element edges, which is enforced through the penalty function method i.e., the edges of two adjacent elements are held together by normal and shear springs.

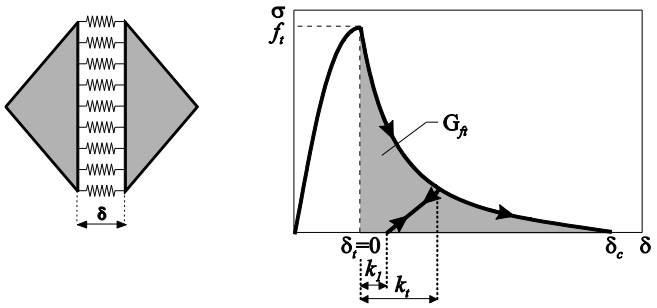

Fig. 4 Strain softening curve defined in terms of displacements

After reaching tensile strength f_t, stress decreases with an increasing separation δ, and at $\delta=\delta_c$ bonding stress tends to zero. For separation $\delta_t<\delta<\delta_c$, bonding stress is given by

$$\sigma_c = z\, f_t \tag{1}$$

where z is a heuristic scaling function representing an approximation of experimental stress-displacement curves (Hordijk 1992),

$$z = \left[1+(c_1 D_t)^3\right] e^{-c_2 D_t} - D_t (1+c_1^3)\, e^{-c_2} \tag{2}$$

where c_1=3, c_2=6,93, and the damage parameter D_t is determined according to the following expression

$$D_t = \begin{cases} (\delta-\delta_t)/(\delta_c-\delta_t), & \text{if} \quad \delta_t < \delta < \delta_c; \\ 1, & \text{if} \quad \delta > \delta_c \end{cases} \tag{3}$$

A similar model for describing shear stress τ_s and shear displacement t_s relation is adopted for concrete behaviour in shear.

In this numerical model, concrete contact element is extended to capture main characteristics related to cyclic loading in tension. For this purpose, material model shown in Fig. 4 is adopted (Reinhardt 1984), where the ratio of k_1/k_t was obtained experimentally from uniaxial cyclic tests and equals to 0,73.

The model of reinforcing bar in the joint element is divided into parts before and after the opening of the crack (Živaljić *et al.* 2013). Before the opening of the crack in concrete, continuity between the reinforcing bar finite elements is ensured through the penalty function method. After the cracking, a path-dependent mechanical model for a deformed reinforcing bar in the joint element (Soltani and Maekawa 2008) is used to describe the behaviour of the reinforcing bar at

crack faces. The model takes into account the bond deterioration in the reinforcement near the crack plane and can accurately express the behaviour of a reinforcing bar that undergoes a high plastic deformation under reversed cyclic loading, and shear force carried by the bar.

The axial tension force developing in the reinforcing bar is partly transferred to the concrete between adjacent cracks through the bonding between the reinforcing bar and concrete. Consequently, the local stress along the bar differs from that at the interface. It causes no uniform distribution of strains along the bar which, among other factors, depends on the bar pull out *S* from the crack interface (Fig. 5) (Soltani and Maekawa 2008, Nikolić *et al.* 2017b).

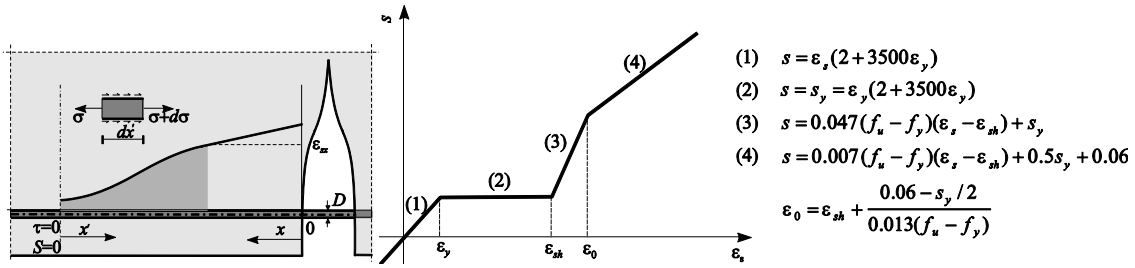

Fig. 5 Discrete crack and steel strain-slip relation under monotonic loading

The monotonic slip-strain relations are defined according to the non-dimensional slip *s* given by

$$s = \left(\frac{S}{D}\right) K_{fc}, \quad K_{fc} = \left(\frac{f_c}{20}\right)^{2/3} \tag{4}$$

where D is the diameter of the bar and f_c is the compressive strength of concrete (MPa). Non-dimensional slip-strain relationship before and after yielding of steel is used according to the expressions shown in Fig. 5, where ε_s represents the strain at the reinforcing bar in the crack, ε_y refers to the yielding strain of the bar, f_u and f_y to the tensile strength and yield stress of steel (MPa) respectively, while ε_{sh} to the strain at the onset of hardening. After yielding of the reinforcing bar, the normalised steel slip s is expressed as the sum of the slip s_{pl} in the yield region and s_e in the elastic region as

$$s = s_{pl} + s_e \tag{5}$$

Assuming a linear distribution of strain in the yield region, the normalised steel slip s_{pl} is expressed as

$$s_{pl} = \frac{(1+\beta)\varepsilon_s + \varepsilon_{sh} - \beta\varepsilon_{\max}}{\varepsilon_{\max} + \varepsilon_{sh}} (s_{\max} - s_y) \tag{6}$$

where $\varepsilon_{\max}$ and $s_{\max}$ represent steel strain and non-dimensional slip immediately after the transition from loading to unloading, and β is a factor obtained from experiments and taken as 1.0. By incorporating equation (5) into (4), the strain in the reinforcing bar at the crack can be obtained from the known non-dimensional slip *s*. The influence of adjacent cracks is approximately taken into account through a reduction factor α (Soltani and Maekawa 2008), which depends on the

average distance between cracks l_{cr}. The steel slip s_{cr}, which considers the influence of adjacent cracks, is expressed for monotonic loading (Živaljić *et al.* 2013). The position of the crack is defined by a finite element edge, so that l_{cr} is adopted as an input parameter, which is equal to $h/2$ where h is the concrete finite element length (Živaljić *et al.* 2014).

3.2 Characteristics of the building and numerical modelling

A five-storey RC building with the uncoupled wall system, shown in Fig. 6, was analysed in order to study the influence of ductility classes on the buildings with wall structural system. The vertical load of the building consists of the weight of its structural elements, an additional dead load of 2.5 kN/m^2 and imposed load of 4.0 kN/m^2 at floor slabs.

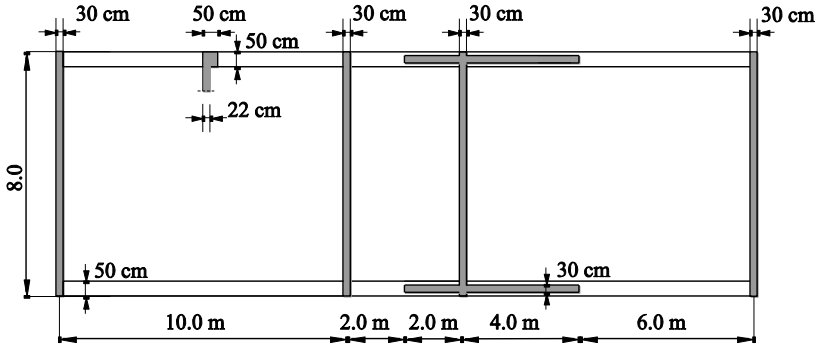

Fig. 6 Geometry of RC building with uncoupled wall system

The building was previously designed according to the regulations of EC8 for importance factor II (γ_I=1), type 1 response spectrum, damping ξ=5%, ground type B, design ground acceleration a_g=0.3 g and ductility classes DCM and DCH. Behaviour factors of q=3.0 for DCM and q=4.4 for DCH are adopted. The linear response spectrum analysis of the whole building was applied firstly in order to calculate internal forces and to design the reinforcement in characteristic cross-sections, considering the design rules of EC8.

The influence of the ductility classes to the behaviour of the structure was analysed by incremental dynamic analysis for the left boundary wall with geometry and reinforcement obtained from previous design (see Fig. 7). The wall was exposed to in-plane earthquake action represented by selected earthquakes and vertical loads consist of the weight of the wall and the load from the corresponding slab surface. The slab loads (dead load, additional dead load and imposed load) from a half of distance between the neighbouring walls, i.e., 5 m, was used and applied at the positions where the wall was connected with the slabs. Material characteristics of concrete and steel are shown in Table 2.

3.3 Incremental dynamic analysis and discussion of the results

The observed boundary RC wall was exposed to in-plane horizontal ground acceleration of selected seven earthquakes (Table 1). The amplitudes were gradually increased, starting with low intensity of acceleration until the collapse of the wall, with an increment a/g=0.02. A large

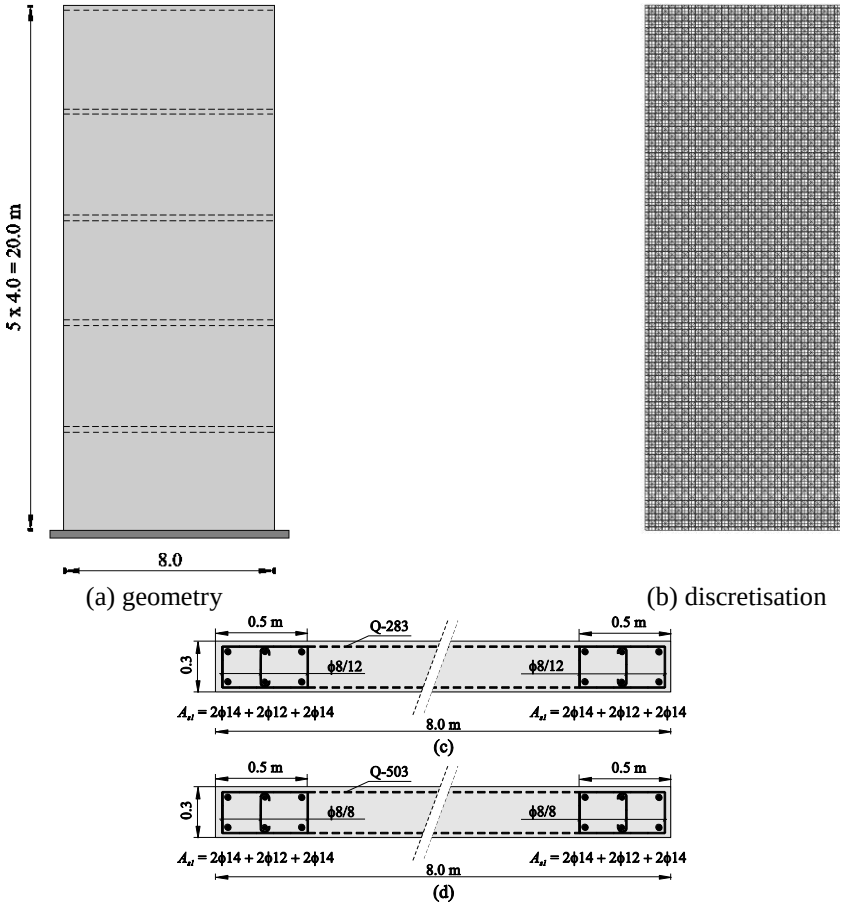

(a) geometry (b) discretisation

(c) DCM wall reinforcement (d) DCH wall reinforcement

Fig. 7 Boundary RC wall

Table 2 Material characteristics of the wall

Concrete					
Young's Modulus E_c / MPa	Poisson's ratio ν	Tensile strength f_t / MPa	Compressive strength f_c / MPa	Fracture energy G_f / N/m	Spatial weight ρ / kN/m^3
32800	0.2	3.80	38	150	25
Steel					
Young's Modulus E_s / MPa	Yield stress f_y / MPa	Ultimate stress f_u / MPa	Strain at onset of hardening ε_{sh}	Ultimate strain ε_u	
210000	500	600	0.02	0.1	

amount of data was obtained from the incremental dynamic analysis hence, for the purpose of brevity, we will discuss the results which are considered the most important features of the structures subjected to seismic loading, such as capacity of the wall, crack pattern and inter-storey

drifts.

Non-linear behaviour of the wall and its seismic capacity for selected earthquakes obtained by incremental dynamic analysis for both ductility classes is shown in Figs. 8 and 9 considering the relation between the peak ground acceleration (*a/g*) and the relative top displacement (*u*/*H*), where *H* is building height.

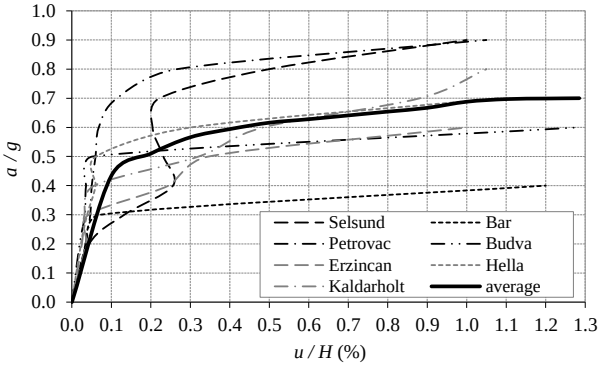

Fig. 8 Curves for relative top displacement (*u/H*), DCM RC wall

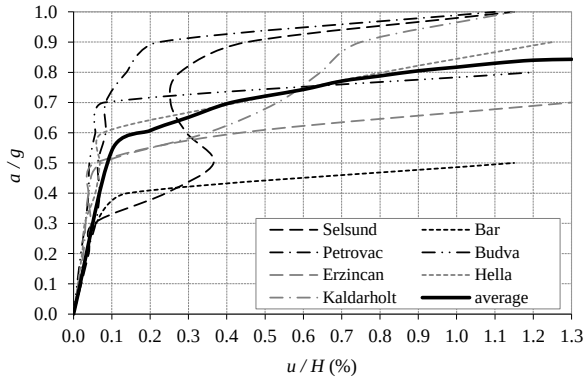

Fig. 9 Curves for relative top displacement (*u/H*), DCH RC wall

Analysis of the average dynamic response of the wall, calculated as a mean value of the responses obtained for seven selected earthquake records, (Figs. 8 and 9) shows that the behaviour of the wall designed for DCM class is linear up to the ground acceleration a=0.30 g. Significant non-linearity starts for a=0.48 g, while the collapse of the wall occurs for a=0.70 g. Wall designed according to DCH is in linear elastic region up to a=0.40 g. Average collapse acceleration a=0.84 g was observed for DCH class.

The most destructive earthquake for both ductility classes is Bar, with ultimate collapse accelerations a=0.40 g and a=0.50 g for DCM and DCH classes respectively. The least destructive earthquakes, considered through the aspect of collapse accelerations, are Petrovac and Selsund, which produced the collapse of the wall for a=0.90 g (DCM) and a=1.0 g (DCH).

It can be observed that the wall reinforced according to DCH possesses average seismic resistance 20% higher with respect to DCM. It is interesting to emphasise that the longitudinal

flexural reinforcement in the boundary elements is the same for both ductility classes in order to meet the requirement of the minimum percentage of reinforcement. The differences pertain to confining reinforcement in boundary elements and web shear reinforcement which caused higher seismic resistance of the high ductility wall. Average responses for both ductility classes still remain linear before the reached design ground acceleration.

Figs. 10 and 11 show crack patterns for DCM and DCH walls exposed to earthquake excitation of Montenegro (aftershock) - Budva. The reason for choosing Budva earthquake is in a fact that this earthquake has response which is near to the average value for considering seven earthquakes. The collapse for this earthquake for DCM and DCH is achieved for accelerations of a=0.60 g and a=0.80 g respectively.

The first cracks for both ductility classes occur for acceleration of a=0.30 g in the bottom part of the wall. Initial horizontal cracks are elongated and connected with each another for a=0.50 g (DCM) and 0.70 g (DCH). The structure is seriously damaged for acceleration a=0.60 g (DCM) and 0.80g (DCH), with a large number of cracks on the first floor of the wall and horizontal cracks on the second and third floors. Cracking patterns reveal rougher cracking with a smaller number of larger cracks in the DCM wall, while fine small crack pattern and crushing of the concrete was noticed for the DCH wall during the collapse acceleration. This is a consequence of reinforcement of the DCH wall with greater amount of confining and shear web reinforcement. It can be noted that a greater amount of embedded confining and shear web reinforcement for DCH contributes not only to a slower development of the cracks, but also to a higher ultimate acceleration.

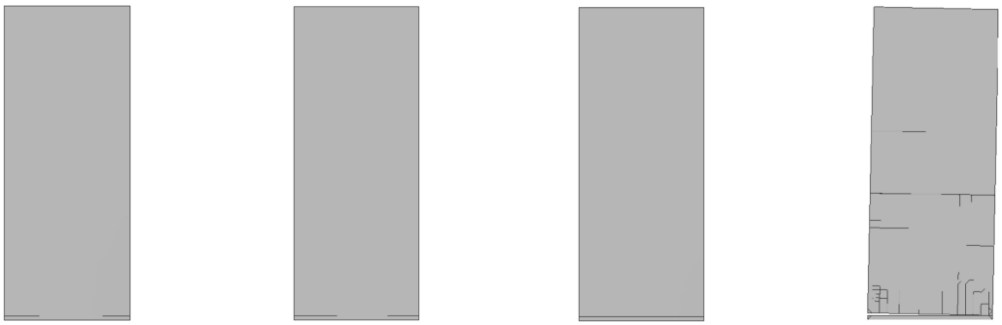

(a) a=0.3 g (b) a=0.4 g (c) a=0.5 g (d) a=0.6 g

Fig. 10 Crack pattern for DCM wall, earthquake Montenegro (aftershock) - Budva

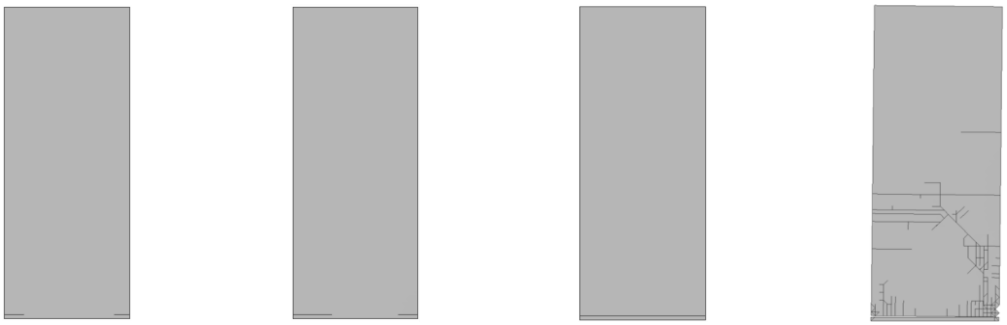

(a) a=0.3 g (b) a=0.4 g (c) a=0.7 g (d) a=0.8 g

Fig. 11 Crack pattern for DCH wall, earthquake Montenegro (aftershock) - Budva

The collapse of the DCM wall occurred due to the fracture of the reinforcing bars, which results in the reduction in lateral stiffness and strength of the wall under seismic loading. The reason of the collapse of DCH walls is crushing under diagonal compression, resulting in a sudden loss of lateral resistance.

Fig. 12 shows the maximum inter-storey drift ratio ($\Delta u/H$) as a function of the ground acceleration, for DCM and DCH walls exposed to seismic excitation with selected earthquakes.

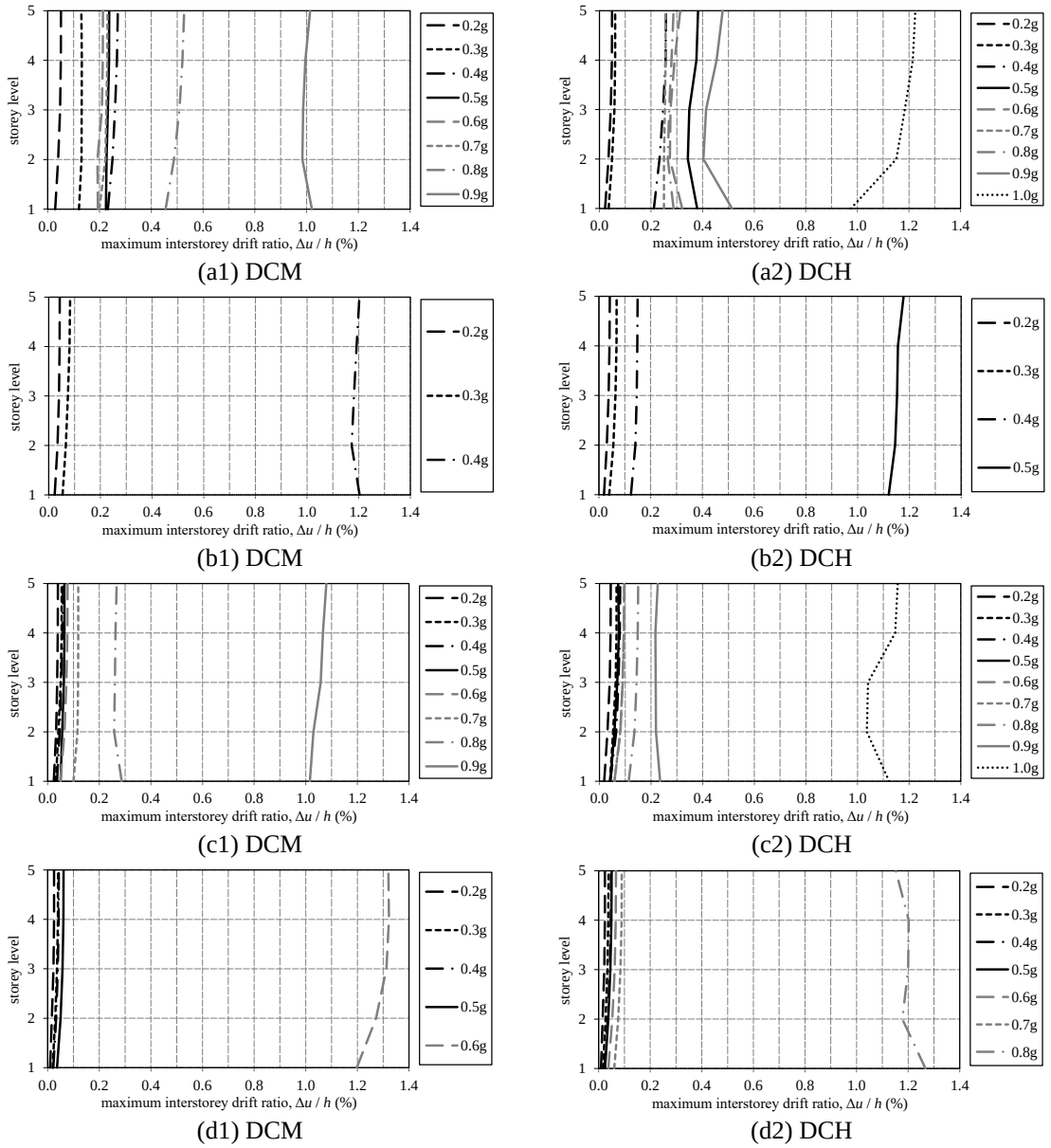

Fig. 12 Maximum inter-storey drifts of DCM and DCH walls for earthquakes: (a) Selsund; (b) Bar; (c) Petrovac; (d) Budva; (e) Erzincan; (f) Hella; (g) Kaldarholt

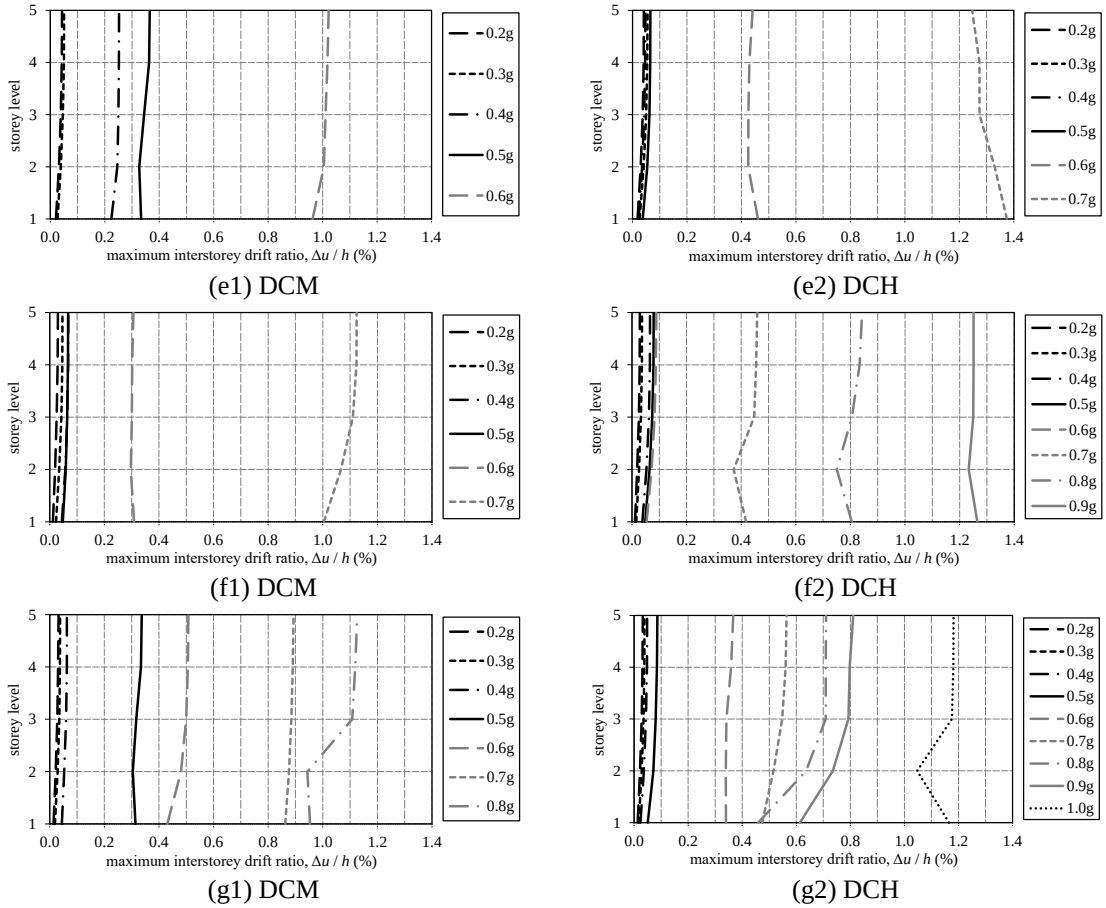

(e1) DCM (e2) DCH

(f1) DCM (f2) DCH

(g1) DCM (g2) DCH

Fig. 12 Continued

Maximum inter-storey drifts present significantly different results with respect to selected earthquakes. Bar and Budva earthquakes cause small inter-storey drifts (less than 0.2%) up to the value which is approximately 80% of the ultimate acceleration. All inter-storey drifts suddenly increase before the wall collapses. Inter-storey drifts for other earthquakes, after small values at the beginning, gradually increase in non-linear region of the structural behaviour up to the collapse acceleration. Maximum inter-storey drift for the DCM wall is obtained for Budva earthquake (1.33%), while Erzincan earthquake causes maximum value for the DCH wall (1.38%).

4. Non-linear analysis of RC frame building

4.1 Description of numerical model

The non-linear time-history analysis of RC frame building was performed by the SeismoStruct programme. Large displacements and rotations and P-Δ effect are taken into account through the employment of a total co-rotational formulation. Material inelasticity and the cross-section

behaviour are presented through the fibre approach, where each fibre is associated with a uniaxial stress-strain relationship. A reinforced concrete section consists of unconfined concrete fibres, confined concrete fibres and steel fibres. Non-linear behaviour of concrete was adopted through non-linear constant confinement model, where the confinement effect is provided by the constant pressure which is caused by lateral transverse reinforcement (Mander *et al.* 1988). Behaviour of steel is modelled by bilinear steel model with kinematic strain hardening. Hysteretic response of both materials is defined by the material constitutive models. The stress-strain relation in the element cross section (beams, columns) can be obtained as a result of the integration of non-linear uniaxial response of the fibres. The dynamic time-history analysis is computed by direct integration of the equations of motion with the Newmark scheme. Modelling of seismic loading is achieved by introducing acceleration loading curves of selected earthquakes.

4.2 Characteristics of the building and numerical modelling

A five-storey RC frame building, regular in the plan and elevation, shown in Fig. 13, was analysed in order to study the influence of the ductility classes on the buildings with frame structural system. The dimensions in the plan are 27x15 m. The bottom storey height equals to 4.0 m, whereas at the other levels it equals to 3.2 m. The cross-section dimensions are 50x50 cm for all columns, and 30x45 cm for all beams. The spans are 6 m and 3 m. The structure has RC slabs with thickness equal to 16 cm. The concrete characteristic cubic strength is f_{ck}=30 N/mm^2, and steel characteristic yielding strength is f_{yk}=500 N/mm^2. The building loads are self-weight, additional dead load of 2.8 kN/m^2 and imposed load of 3.0 kN/m^2.

The building was previously designed according to the regulations of EC8 for importance factor II (γ_I=1), type 1 response spectrum, damping ξ=5%, ground type B, design ground acceleration a_g=0.3 g and ductility classes DCM and DCH. Behaviour factors equal to q=3.9 for DCM and q=5.85 for DCH are adopted. The linear response spectrum analysis was applied in order to calculate internal forces and reinforcement in characteristic cross-sections as a result of earthquake action to the building.

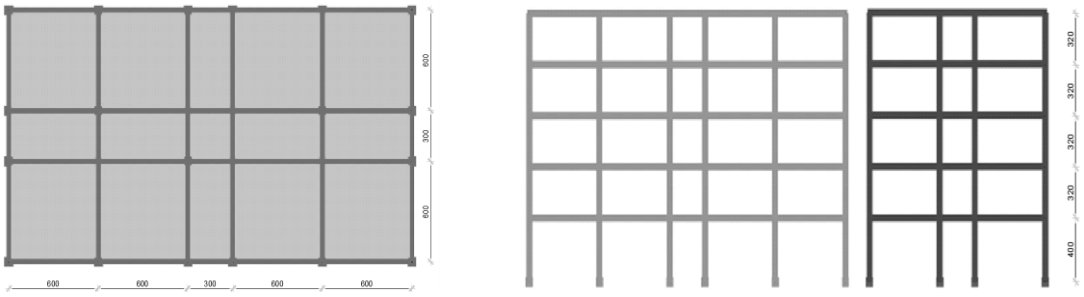

(a) Plan (b) Section

Fig. 13 Geometry of the building

DCM frame was designed with columns reinforced by 20ϕ18, 4ϕ10/10 cm stirrups in critical region and ϕ8/20 cm stirrups out of critical region, whereas the beams were reinforced by longitudinal 7ϕ18 bars in upper and lower section, and ϕ8/15 cm stirrups.

DCH frame was designed with the columns reinforced by longitudinal 24ϕ16 bars, 4ϕ10/10 cm stirrups in critical region, and ϕ8/20 cm stirrups out of critical region. The beams have longitudinal 7ϕ16 bars in upper and lower section, and ϕ8/15 cm stirrups. Special attention was devoted to the design of beam-column connections which are very susceptible to damage during the earthquake event (Domínguez and Pérez-Mota 2014). Therefore, the additional horizontal ϕ10/5 cm bars were placed in beam-column joints to ensure ductility behaviour.

The influence of the plate to flexural and torsional stiffness was taken by modelling the beams as T cross-section with effective width of 80 cm.

4.3 Incremental dynamic analysis and discussion of the results

The differences in behaviour for both ductility classes was analysed by incremental dynamic analysis performed on inner RC plane frame with geometry and reinforcement obtained from previous seismic design. In this analysis, SeismoStruct programme was used, as already mentioned in section 4.1. The frame was exposed to earthquake action and vertical loads consist of the weight of the frame and the load from the corresponding slab surface. The slab loads (dead load, additional dead load and imposed load) from a half of distance between the neighbouring frames, i.e., 1.5+3.0=4.5 (m), was used and applied at the beams.

Each of the chosen seven records (Table 1) was applied with increasing ground motion intensity up to the structural collapse. Figs. 14 and 15 shows response curves of the frame, designed for DCM and DCH respectively, for selected earthquakes considering the relation between the peak ground acceleration (*a/g*) and the relative top displacement (*u/H*), where *H* is building height.

The most destructive earthquake, considering the collapse acceleration for both ductility classes, is Budva, with ultimate collapse accelerations *a*=0.29 *g* and *a*=0.30 *g* for DCM and DCH classes respectively. The least destructive earthquakes are Kaldarholt with collapse acceleration *a*=0. 41 *g* (DCM) and *a*=0.36 *g* (DCH) and Selsund which produced the collapse of the frame for *a*=0.37 *g* (DCM) and *a*=0.35 *g* (DCH).

The average collapse acceleration of *a*=0.36 was observed for DCM frame, while DCH frame achieved *a*=0.33 *g* at the failure stage. The frame reinforced according to the DCM possesses average seismic resistance 11% higher with respect to DCH.

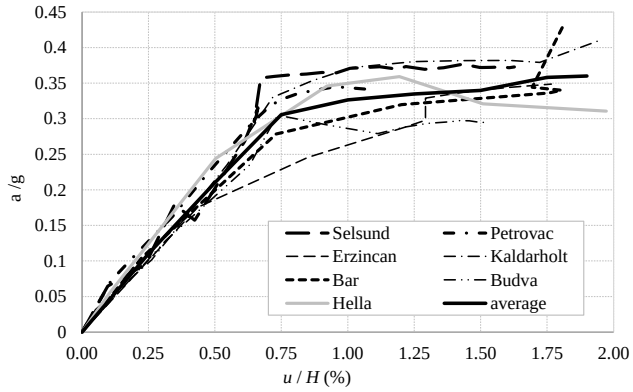

Fig. 14 Curves for relative top displacement (*u/H*), DCM frame

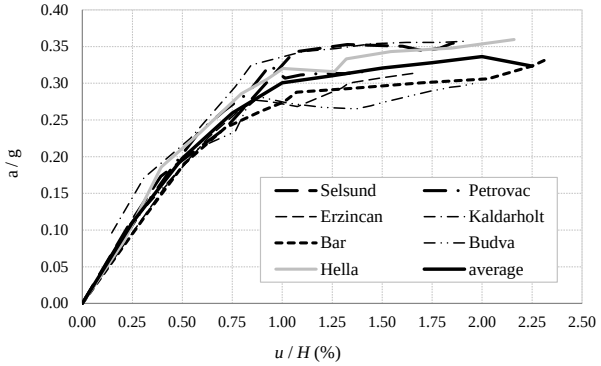

Fig. 15 Curves for relative top displacement (*u/H*), DCH frame

In this example, there was no significant difference between the bearing capacity of DCM and DCH frames, because the reinforcement embedded in the columns of the DCM frame was slightly larger than in the DCH frame. In fact, the DCH frame was designed for lower lateral strength, and it was expected that its seismic resistance is considerably lower, 50% lower on average, due to a higher behaviour factor. Meeting the requirements to design the primary seismic columns stronger than the beams, with an overstrength factor of 1.3 on beam design flexural capacities, results in having the columns in DCH frames with similar flexural capacity as in the DCM frame. Therefore, seismic resistance of both frames represented through collapse acceleration does not significantly differ.

Fig. 16 shows damage of the frames exposed to earthquake excitation of Montenegro (aftershock)-Budva which occurred for a=0.29g (DCM) and a=0.30g (DCH). Adopted model used the following yielding and failure criteria: reinforcement yielding (red colour in Fig. 16) is achieved for deformation of 0.25%, reinforcement failure (green) for deformation of 6%, crushing of the concrete protective layer (blue) for deformation of 0.35% and crushing of the concrete core (black) for deformation of 0.8%.

The frame reinforced according to DCM ductility class shows the yielding of the reinforcing bars in the beams critical regions of the first and second floors, as well as in the columns` lower critical regions of the first, second and third floors. Reinforcement failure and crushing of the concrete protective layers occur in the basis of the columns.

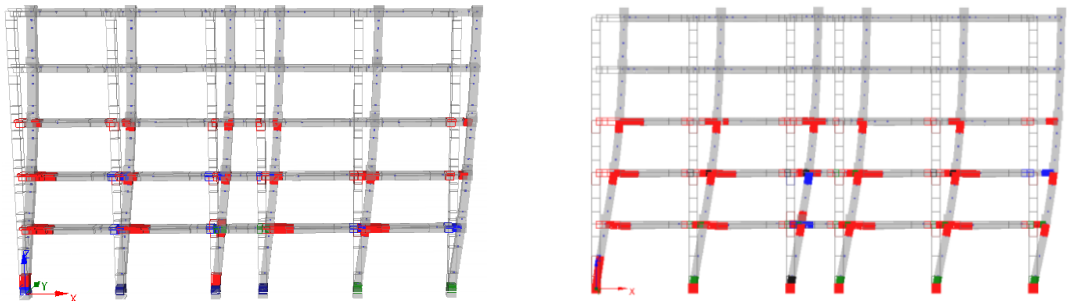

(a) DCM (b) DCH

Fig. 16 Damage of the structure, Montenegro earthquake (aftershock) - Budva

Several types of damages occurred for the frame designed according to DCH ductility class, including the crushing of the concrete protective layer and concrete core in the columns of the first floor, expansion of plastic zones in the beams and further propagation of plastification in the columns of the third floor.

5. Conclusions

• In this paper, the behaviour of RC buildings, previously designed for DCM and DCH ductility class according to the regulations of EC8, was analysed by using incremental dynamic analysis in order to study the differences in the behaviour of the structure between these ductility classes, especially the collapse mechanism and collapse loads. The analyses were performed for design acceleration of 0.30*g* and seven time-history records of earthquakes, which were chosen to satisfy the acceleration spectrum assumed in the design.

• RC building with wall structural system was designed for lower lateral strength in the case of ductility class DCH, so it was expected that its seismic resistance is considerably lower, in comparison to DCM class, due to a higher behaviour factor. But finally, the walls had the same longitudinal flexural reinforcement in the boundary elements for both ductility classes by meeting the requirements of the minimum percentage of reinforcement. The differences pertaining to confining reinforcement in boundary elements and web shear reinforcement caused higher average seismic resistance of the DCH wall. The average collapse of DCM and DCH walls occurred for acceleration of a=0.70*g* and a=0.84*g*, respectively. The ultimate collapse acceleration for different earthquakes varied from 0.4*g* to 1.0*g*, and it was mainly significantly higher than the design acceleration. The cracking patterns reveal rougher cracking with a smaller number of larger cracks in the DCM wall, whereas fine small crack pattern and crushing of the concrete was noticed for the DCH wall during the collapse acceleration. The collapse of the DCM wall occurred due to the fracture of the reinforcing bars which results in the reduction in lateral stiffness and strength of the wall. The reason of the collapse of DCH walls is crushing under diagonal compression, resulting in a sudden loss of lateral resistance.

• RC frame building of DCH ductility class was also calculated for lower lateral strength than DCM building. Similar as in the wall building, significantly lower resistance of the DCH frame was expected. Finally, the longitudinal reinforcement of the beams in critical region was 27% higher for ductility class DCM in comparison to DCH, but the longitudinal reinforcement of the columns is only 6% higher for DCM. The reason for the small difference in the percentage of reinforcement between two classes is in meeting the requirements to design the primary seismic columns to be stronger than the beams, with an overstrength factor of 1.3 on beam design flexural capacities. Therefore, the columns in DCH frames had a slightly lower flexural capacity in comparison to the DCM frame. The seismic resistance of both frames represented through collapse acceleration does not significantly differ, i.e. resistance of the frame for DCM is 11% higher in relation to DCH. The failure mechanisms are very similar for both classes. After the yielding of the reinforcement in the beam-column joint, the collapse for both ductility classes occurred due to the crushing of the concrete and reinforcement failure in the basis of the columns. Strong columns and weak beams produced plastification of the beams in the beam-column joints firstly, as it was expected when the design and detailing rules of EC8 were strictly applied. The ultimate collapse accelerations were 20-25% higher than the design acceleration.

• Presented conclusions are derived from an analysis of only two RC wall buildings, one with

wall and the other with frame structural system. We cannot say that derived conclusions are generally applicable to all RC structures. Further analysis of a number of structures are necessary to determine the differences in behaviour between the two ductility classes and the purposefulness of the design for DCH ductility class, considering that the design effort required for DCH structures is more demanding, and sometimes the detailing provisions are found hard to achieve in practice.

Acknowledgments

This work has been fully supported by Croatian Science Foundation under the project *Development of numerical models for reinforced-concrete and stone masonry structures under seismic loading based on discrete cracks* (IP-2014-09-2319).

References

Armero, F. and Garikipati, K. (1996), "An analysis of strong discontinuities in multiplicative finite strain plasticity and their relation with the numerical simulation of strain localization in solids", *J. Sol. Struct.*, **33**, 2863-2885.

Armero, F. and Linder, C. (2009), "Numerical simulation of dynamic fracture using finite elements with embedded discontinuities", *J. Fract.*, **160**, 119-141.

Bažant, Z.P., Caner, F., Adley, M. and Akers, S. (2000), "Fracturing rate effect and creep in microplane model for dynamics", *J. Eng. Mech.*, **126**(9), 962-970.

Boot, E. (2014), *Earthquake Design Practice for Buildings*, 3rd Edition, Thomas Telford Limited, London, U.K.

Cusatis, G., Bažant, Z.P. and Cedolin, L. (2006), "Confinement-shear lattice CSL model for fracture propagation in concrete", *Comput. Meth. Appl. Mech. Eng.*, **195**(52), 7154-7171.

D'Addetta, G.A., Kuhl, E., Kun, F. and Ramm, E. (1999), "Micromechanical modelling of concrete cracking", *Proceedings of the European Conference on Computational Mechanics*, Munich, Germany.

Domínguez, N. and Pérez-Mota, J. (2014), "Coupling of nonlinear models for steel-concrete interaction in structural RC joints", *Coupled Syst. Mech.*, **3**(2), 195-211.

Eurocode 8 (2005), *Design of Structures for Earthquake Resistance-Part 1: General Rules, Seismic Actions and Rules for Buildings*, EN 1998-1, CEN, Brussels.

European Strong-Motion Database, <http://www.isesd.hi.is>.

Ghaboussi, J. (1997), "Fully deformable discrete element analysis using a finite element approach", *J. Comput. Geotech.*, **5**,175-195.

Hordijk, D.A. (1992), "Tensile and tensile fatigue behaviour of concrete-experiments, modelling and analyses", *Heron*, **37**(1), 3-79.

Ibrahimbegovic, A., Boulkertous, A., Davenne, L. and Brancherie, D. (2010), "Modelling of reinforced-concrete structures providing crack-spacing based on X-FEM, ED-FEM and novel operator split solution procedure", *J. Numer. Meth. Eng.*, **83**, 452-481.

Iervolino, I., Maddaloni, G. and Cosenza, E. (2008), "Eurocode 8 compliant real record sets for seismic analysis of structures", *J. Earthq. Eng.*, **12**, 54-90.

Mander, J.B., Priestley, M.J.N. and Park, R. (1988), "Theoretical stress-strain model for confined concrete", *J. Struct. Eng.*, **114**(8), 1804-1826.

Moës, N., Dolbow, J. and Belytschko, T. (1999), "A finite element method for crack growth without remeshing", *J. Numer. Meth. Eng.*, **46**, 131-150.

Munjiza, A. (2004), *The Combined Finite-Discrete Element Method*, John Wiley & Sons, London, U.K.

Nam Do, X., Ibrahimbegovic, A. and Brancherie, D. (2015a), "Combined hardening and localized failure

with softening plasticity in dynamics", *Coupled Syst. Mech.*, **4**(2), 115-136.
Nam Do, X., Ibrahimbegovic, A. and Brancherie, D. (2015b), "Localized failure in damage dynamics", *Coupled Syst. Mech.*, **4**(3), 211-235.
Nikolic, M. and Ibrahimbegovic, A. (2015), "Rock mechanics model capable of representing initial heterogeneities and full set of 3D failure mechanisms", *Comput. Meth. Appl. Mech. Eng.*, **290**, 209-227.
Nikolic, M., Ibrahimbegovic, A. and Miscevic, P. (2015), "Brittle and ductile failure of rocks: Embedded discontinuity approach for representing mode I and mode II failure mechanisms", *J. Numer. Meth. Eng.*, **102**(8), 1507-1526.
Nikolic, M., Ibrahimbegovic, A. and Miscevic, P. (2016), "Discrete element model for the analysis of fluid-saturated fractured poro-plastic medium based on sharp crack representation with embedded strong discontinuities", *Comput. Meth. Appl. Mech. Eng.*, **298**, 407-427.
Nikolic, M., Karavelic, E., Ibrahimbegovic, A. and Miscevic, P. (2017a), "Lattice element models and their peculiarities", *Archiv. Comput. Meth. Eng.*
Nikolić, Ž., Živaljić, N., Smoljanović, H. and Balić, I. (2017b), "Numerical modelling of reinforced-concrete structures under seismic loading based on the finite element method with discrete inter-element cracks", *Earthq. Eng. Struct. Dyn.*, **46**(1), 159-178.
Ortiz, M. and Pandolfi, A. (1999), "Finite-deformation irreversible cohesive elements for three-dimensional crack-propagation analysis", *J. Numer. Meth. Eng.*, **44**, 1267-1282.
Ortiz, M. and Quigley, J.J. (1991), "Adaptive mesh refinement in strain localization problem", *Comput. Meth. Appl. Mech. Eng.*, **90**, 781-804.
Ožbolt, J., Li, Y. and Kožar, I. (2001), "Microplane model for concrete with relaxed kinematic constraint", *J. Sol. Struct.*, **38**(16), 2683-2711.
Pearce, C.J., Thavalingam, A., Liao, Z. and Bićanić, N. (2000), "Computational aspects of the discontinuous deformation analysis framework for modelling concrete fracture", *Eng. Fract. Mech.*, **65**, 283-298.
Pramanik, D., Banerjee, A.K. and Roy, R. (2016), "Implications of bi-directional interaction on seismic fragilities of structures", *Coupled Syst. Mech.*, **5**(2), 101-126.
Reinhardt, H.V. (1984), "Fracture mechanics of an elastic softening material like concrete", *Heron*, **29**(2), 3-41.
Rethore, J., Gravouil, A. and Combescure, A. (2005), "An energy-conserving scheme for dynamic crack growth using the eXtended finite element method", *J. Numer. Meth. Eng.*, **63**(5), 631-659.
Schlangen, E. and Garboczi, E.J. (1997), "Fracture simulation of concrete using lattice models: computational aspects", *Eng. Fract. Mech.*, **57**(2/3), 319-332.
SeismoStruct, *A Computer Program for Static and Dynamic Nonlinear Analysis of Framed Structures*, <http://www.seismosoft.com>.
Simo, J.C., Oliver, J. and Armero, F. (1993), "An analysis of strong discontinuities induced by strain-softening in rate-independent inelastic solids", *Comput. Mech.*, **12**, 277-296.
Soltani, M. and Maekawa, K. (2008), "Path-dependent mechanical model for deformed reinforcing bars at RC interface under coupled cyclic shear and pullout tension", *Eng. Struct.*, **30**, 1079-1091.
Vamvatsikos, D. and Cornell, C.A. (2002), "Incremental dynamic analysis", *Earthq. Eng. Struct. Dyn.*, **31**, 491-514.
Wells, G.N., Sluys, L.J. and Borst, R. (2002), "Simulating the propagation of displacement discontinuities in a regularized strain-softening medium", *J. Numer. Meth. Eng.*, **53**, 1235-1256.
Yamamoto, Y., Nakamura, H., Kuroda, I. and Furuya, N. (2014), "Crack propagation analysis of reinforced concrete wall under cyclic loading using RBSM", *Eur. J. Environ. Civil Eng.*, **18**(7), 780-792.
Živaljić, N., Nikolić, Ž. and Smoljanović, H. (2014), "Computational aspects of the combined finite-discrete element method in modelling of plane reinforced concrete structures", *Eng. Fract. Mech.*, **131**, 669-686.
Živaljić, N., Smoljanović, H. and Nikolić, Ž. (2012), "Sensitivity analysis of numerical parameters in FEM/DEM model for RC structures", *J. Eng. Modell.*, **25**(1-4), 7-17.
Živaljić, N., Smoljanović, H. and Nikolić, Ž. (2013), "A combined finite-discrete element model for RC structures under dynamic loading", *Eng. Comput.*, **30**, 982-1010.